Towards the production of oxalate precursors from NMC111 black mass via selective leaching of Li and Al and solvent extraction of Cu

Journal of Power Sources Advances 37 (2026) 100201

Contents lists available at ScienceDirect

Journal of Power Sources Advances

journal homepage: www.sciencedirect.com/journal/journal-of-power-sources-advances

Towards the production of oxalate precursors from NMC111 black mass via selective leaching of Li and Al and solvent extraction of Cu

Léa Marie Jacqueline Rouquette [a,*], Laura Altenschmidt [b], Camille Travert [a], Andrea Locati [a], William R. Brant [b], Martina Petranikova [a]

[a] Department of Chemistry and Chemical Engineering, Industrial Materials Recycling and Nuclear Chemistry, Chalmers University of Technology, Gothenburg, Sweden
[b] Department of Chemistry-Ångström, Uppsala University, Uppsala, Sweden

ARTICLE INFO

Keywords:
Recycling
Oxalic acid
Lithium-ion battery
Hydrometallurgy
Cathode active material

ABSTRACT

A novel recycling route for spent lithium-ion batteries has been investigated. The end goal is to produce cathode active material (CAM) precursor directly from the recycled solution. The process begins with an oxalic acid leaching (0.6 M $H_2C_2O_4$, 60 °C, 120 min, and S/L = 50 g/L), where Li is selectively recovered (along with Al) which reduces downstream contamination and enhances overall material efficiency. The resulting residue, a mixture of $(Co,Ni,Mn)C_2O_4 \cdot 2H_2O$, graphite, and Cu, is then leached with sulfuric acid to dissolve the metals and separate them from the graphite. This second leaching operation is investigated, and the optimum parameters are demonstrated (2 M H_2SO_4, 65 °C, 120 min, S/L = 20 g/L), yielding more than 95 % recovery of Ni, Co, and Mn and about 70 % of Cu. Lower acidity or S/L leads to the reprecipitation of a Ni oxalate phase. Solvent extraction is selected for Cu removal at a limit of 5 ppm; a 30 % v/v Acorga M5640 in ESCAID is applied for 30 min at 25 °C, with θ = 4 and 4 stages. The resulting recycled solution, containing Co, Ni, and Mn, and free from Al, Li, and Cu, represents a promising feedstock for producing NMC 111 ($LiNi_{0.33}Mn_{0.33}Co_{0.33}O_2$).

1. Introduction

Lithium-ion batteries (LiBs) are widely used in electronics and electric vehicles (EVs) [1–3], driving up demand for critical raw materials like Li, Co, Cu, Mn, and Ni [1,4,5]. EV batteries are significantly larger than those in portable devices [6], intensifying environmental concerns across the LiB lifecycle, from mining to disposal [1,7–9]. To address these issues, the EU has implemented a battery regulation (No 2023/1542) mandating high recovery rates for critical metals by 2031 [10]. LiBs consist of interconnected cells, each containing alternating layers of cathode, separator, and anode, soaked in liquid electrolyte [1,11,12]. The most spread cathode active materials (CAM) are $LiNi_{0.33}Mn_{0.33}Co_{0.33}O_2$ (NMC), $LiNi_{0.33}Co_{0.33}Al_{0.33}O_2$ (NCA), and $LiFePO_4$ (LFP) [2]. Recycling methods have shifted from energy-intensive pyrometallurgy to hydrometallurgy, which offers higher recovery rates and lower emissions [8,13–19]. The process involves discharging, dismantling, and the black mass (BM) production [20], followed by chemical leaching typically with sulfuric acid and hydrogen peroxide [16,21–23] and separation/purification of metals [14,24–28]. Final recovery steps include precipitation of lithium carbonate, though waste byproducts and emissions remain challenges. Research continues to enhance the circular use of critical minerals, minimize the environmental impact of recycling, and support a more sustainable and resilient supply chain [29]. For instance, the IEA states in its latest report that next-generation leaching (or solvent extraction) techniques should be based on a selective leaching approach with maximized recovery [1], while the EU underscores the importance of employing Best Available Techniques for battery waste treatment [10].

This work is part of a larger initiative to develop a more sustainable and circular process using eco-friendly chemicals like organic acids. The key innovation of the process is the production of NMC cathode material from recycled solutions. Such approach would significantly reduce the number of stages required for metal recycling and enable direct production of CAM precursor (p-CAM) from the recycled solution, eliminating the need for separation into pure compounds and thereby promoting a circular value chain for materials and closing the recycling loop. To achieve this goal, Li is selectively removed by oxalic acid (OA) leaching, which can mitigate its losses throughout the process [30,31].

This article is part of a special issue entitled: Battery Recycling published in Journal of Power Sources Advances.

* Corresponding author.
E-mail address: malea@chalmers.se (L.M.J. Rouquette).

https://doi.org/10.1016/j.powera.2026.100201
Received 29 September 2025; Received in revised form 11 December 2025; Accepted 3 January 2026
Available online 13 January 2026

This work focuses on handling the primary solid residue and investigating this new chemical system. Sulfuric acid is chosen as a leaching media as oxalate complexes are known to be strong and require strong acids to dissolve [32]. This step enhances the separation of graphite and the production of a solution containing all transition metals (TM). Cu removal is investigated by solvent extraction with Acorga M5640 (a commercial extractant). Although the extractant system is known, it has not been tested on such an aqueous solution. Cu removal is essential as its presence negatively affects the CAM performance. Subsequent NMC precursor synthesis is considered but not investigated in this paper.

2. Materials and methods

2.1. Material

Battery packs were discharged and dismantled to reach the battery cell level (Volvo Cars AB and Stena Recycling AB, Sweden). The resulting cells were crushed and sorted by mechanical sieving and magnetic separation below 50 °C to obtain BM powder (Akkuser Oy, Finland). Finally, in-house sieving was performed under 500 μm using a sieve shaker (Retsch - 5 min with interval mode and amplitude 1.2) at room temperature.

2.2. Analytical methods

An inductively coupled plasma-mass spectrometer (ICP-OES, Thermo Fisher Scientific, Model iCAP™ 6000 Series) was used to measure metal concentration. The samples were diluted with 0.5 M HNO_3 to fit the 0.625–20 mg/L calibration range (LOD ≈ 0.3 mg/L). The pH was measured during the operation using a pH electrode (Metrohm 6.0258.600) connected to the Tiamo software to record the data. The electrode was calibrated with buffer solutions at pH 2, 4, and 7 before each experiment at 22 °C ± 1 °C.

The metal composition was determined after aqua regia digestion (3:1 HCl:HNO_3, Merck Millipore, ACS Reagents). About 0.2 g of the solid sample was mixed with the aqua regia at 80 °C for 4 h. The sampling was performed following the coning and quartering method, which is known to decrease uncertainties associated with taking a small portion of the powder bulk [33]. After filtration (Filter VWR 516–0811 - 11 μm particle retention) and dilution, the cold slurry was analyzed via ICP-OES. X-ray diffraction (XRD, Bruker D8 Twin-Twin diffractometer) was performed over the 2θ range of 10°–80° with a rotational speed of 15 rpm using Cu-K_α radiation. Analysis of the XRD data was carried out using the Pawley method in the TOPAS software V6 [34].

An UV/Vis Spectrometer (Lambda 25, PerkinElmer) was used to measure the absorbance over the 900 - 300 nm range. Fourier-transform infrared spectra were recorded from 4000 to 450 cm^{-1} with a resolution of 2 cm^{-1} in ATR mode (Spectrum Two, PerkinElmer).

2.3. Leaching experiments

The OA ($H_2C_2O_4 \cdot 2H_2O$, Sigma Aldrich, ACS Reagent plus, ≥99 %) leaching was performed in a 2 L double-jacked glass reactor with a mechanical overhead stirrer and heating bath. The preliminary investigation of the sulfuric acid (H_2SO_4, Sigma Aldrich, ACS Reagent, 95–98 %) leachings (Section 3.2.1) was performed in PVDF-closed double-jacked reactors with an initial volume of 50 mL. Then, the operation was scaled up (Section 3.2.2), and the leachings were performed in a 1L double-jacked glass reactor equipped with a mechanical head stirrer and heating bath.

In all cases, the proper amount of solid was inserted once the desired temperature was reached. To follow the metal dissolution in the leachate, 1 mL samples were taken from the top during the operation at different times. The slurry was directly filtered (Syringe filter PTFE - Restek – 0.45 μm), and the metal concentration was measured following the abovementioned procedure. The leaching yield (Y_E) was computed using Equation (1):

$$Y_E\ (\%) = \frac{m_{E,liq,t}}{m_{E,BM,0}} = \frac{[E]_t * V_t}{wt\%_E * m_{BM,0}} \quad (1)$$

In which $m_{E,BM,0}$ is the initial mass of the element E in the BM, and $m_{E,liq,t}$ is the mass of the element transferred in the leaching solution after a certain time, t, calculated with the concentration of this element ($[E]_t$) and the volume of the leaching solution (V_t).

2.4. Precipitation experiments

To assess leaching solution stability, 50 mL was placed in an Erlenmeyer flask at room temperature (22 ± 1 °C), and the pH was adjusted using 10 M NaOH. The solution was stirred for 6 h, with samples taken at 1, 2, 4, and 6 h. Oxalate precipitation was observed during and after stirring, with concentrations stabilizing after 72 h. Final concentrations were measured by ICP-OES following filtration.

2.5. Solvent extraction experiments

Batch experiments for Cu extraction were carried out in 3.5 mL glass vials; they were shaken at 1000 rpm for 15 min under constant temperature (25 °C ± 1 °C) using a shaking machine (VXR basic Vibrax®). The organic phase is composed of the extractant, Acorga M5640 (a hydroxy oxime-type organic acid extractant) diluted in ESCAID 100 (hydrocarbon-based solvent – kerosine, petroleum). All experiments were triplicates. The initial pH was measured and controlled. Sampling was performed after satisfactory phase separation and metal concentration in the aqueous phase was measured. The parameters allowing maximal Cu loading, such as the extractant concentration, contacting time, and temperature, were investigated. The extraction percentage was calculated using Equation (2), which relies on the elemental mass balance of the operation.

$$\%E_M = \frac{\overline{[M]_t}}{[M]_0} = \frac{[M]_0 - [M]_t}{[M]_0} = \frac{100 \cdot D_M}{D_M + {}^1/_\theta} \quad with\ D_M = \frac{\overline{[M]_{tot}}}{[M]_{tot}} \quad (2)$$

It quantifies the transfer of the metal, M, initially present in the aqueous phase ($[M]_0$) into the organic phase ($\overline{[M]_t}$) after a specific time, t. θ is the volume ratio between the organic phase (V_{org}) and the aqueous phase (V_{aq}). The distribution ratio, marked D, describes the metal partition between the two phases. It is computed as the total metal concentration in the organic phase ($\overline{[M]_{tot}}$) over the total metal concentration in the aqueous phase ($[M]_{tot}$), usually measured at equilibrium.

3. Results and discussion

The BM was leached at 60 °C for 120 min with OA at 0.6 M at an initial fixed Solid/Liquid (S/L) ratio of 50 g/L as reported in our previous research [30]. The CAM reacts with oxalic acid following Equation (3). The leaching yields of every element during the operation are shown in Fig. S1a (100 % of Al and 85 % of Li dissolved). The XRD of the residue (Fig. S1b) reveals that the leaching residue is mainly composed of a disordered $(Co,Ni,Mn)C_2O_4 \cdot 2H_2O$ phase, graphite, and Cu [31]. Fig. S2 provides more characterization of this residue. Thorough characterization is essential as this Leaching I residue was used as feed material in the next leaching step (Leaching II).

$$LiCo_xNi_yMn_zO_{2(s)} + 2\ H_2C_2O_{4(aq)} = {}^1/_2\ Li_2C_2O_{4(aq)} + (Co_xNi_yMn_z)C_2O_4 \cdot 2H_2O_{(s)} + CO_{2\ (g)} \quad (3)$$

3.1. Sulfuric acid leaching (leaching II)

3.1.1. Preliminary experiments

Sulfuric acid is applied as the leaching media; the objective is to dissolve the metallic content from the oxalate residue and leave the

graphite behind. Simple oxalates ($MC_2O_4 \cdot xH_2O$) are strong complexes, insoluble in water, but are reported to dissolve in strong acidic conditions [35]. Preliminary experiments were performed to assess the main parameters (temperature, molarity, and S/L ratios) affecting the dissolution of the mixed oxalate phase, before continuing a deeper investigation of the leaching mechanism.

The leaching yields obtained for each element are depicted in Fig. 1a–c. Li shows complete dissolution regardless of the experimental conditions chosen; the form in which it was left in the residue is easily soluble. Co and Mn demonstrate good dissolution behavior, while Ni and Cu dissolve, on average, 20 % less.

As the temperature positively affects the dissolution of every metal, with an approximate increase of 30 % recovery of Co and Mn when increasing the temperature from 50 to 80 °C, and only 10 % for Ni and Cu (Figs. 1a), 65 °C was selected for the rest of the experiments.

Both acidity and the S/L ratio are critical and interdependent parameters in the process, influencing chemical equilibrium and mass transfer. Higher acidity enhances the metallic dissolution, while a lower S/L ratio further promotes it by increasing the availability of solvent relative to the solid (Fig. 1b–c). To determine the optimal combination of the acidity level and the S/L ratio and to compare their cumulative impact, Fig. 1d was plotted. For this, the S/L ratio and the acidity are computed together as one parameter: the molar ratios between the number of moles of acidity available for the total number of moles of metals in the residue (n_{Acid}:$n_{Tot\ Metals}$, with the metals considered: Co, Ni, Mn, Li, and Cu). Consistently, the higher the molar ratio, the more metal is dissolved in the solution. The trend is sensibly positive, and about 80 % of Co and Mn are dissolved when applying a minimum of 2 M H_2SO_4 with an S/L ratio below 80 g/L, corresponding to a molar ratio of 5. Nevertheless, one interesting aspect is that the curve flattens for the molar ratio between 8 and 12, corresponding to the same S/L ratios (50 g/L) but different molarities of H_2SO_4, respectively 2 M and 3 M. Thus, 2 M H_2SO_4 appears to be of sufficient acidity to dissolve the formed TM oxalate from Leaching I, and this molarity is applied for the rest of the leaching investigation. It is also more advantageous for the overall impact of the process: lower required acidity means lower chemical consumption, lower environmental impact, and improved safety.

Thermodynamics calculations (using HSC Chemistry 10) were performed to determine the spontaneity of the dissolution reaction and to help discuss the observed yield. The reaction equations considered are presented in Table 1. Different reactions were considered: the dissolution of the solid complexes in water (Equations (5)and (8)), in H_2SO_4 (Equations (6) and (9)), and the reaction of the oxalate complexes (solid or not) with the sulfuric acid forming sulfate in solution (Equations ((4), (7), (10) and (11)). Table S1 provide all computed entropies, enthalpies, and Gibbs free energies at various temperatures. Only the solid simple oxalates of Ni and Co are present in the database, whereas only the soluble form of Mn and Cu simple oxalates are available. Consequently, Ni and Co are particularly relevant for this study, as they present the most complete dataset.

The reaction between the solid TM oxalate and H_2SO_4, forming the sulfate-associated species, is spontaneous, i.e. negative ΔG. In contrast, the dissolution of the solid complexes in sulfuric acid or water, forming

Table 1
Thermodynamic consideration – computed with HSC Chemistry 10 with standard states (1 M, 1 atm) and 65 °C.

Reaction Equations	ΔG(65 °C) (kJ/mol)
$CoC_2O_4.2H_2O_{(s)} + H_2SO_{4\ (aq)} \rightleftarrows CoS\ O_{4\ (aq)} + H_2C_2O_{4\ (aq)} + 2H_2O$ (4)	−41.1
$CoC_2O_4.2H_2O_{(s)} + H_2O \rightleftarrows CoC_2O_{4\ (aq)} + 3H_2O$ (5)	27.1
$CoC_2O_4.2H_2O_{(s)} + H_2SO_{4\ (aq)} \rightleftarrows CoC_2O_{4\ (aq)} + H_2SO_{4\ (aq)} + 2H_2O$ (6)	27.2
$NiC_2O_4.2H_2O_{(s)} + H_2SO_{4\ (aq)} \rightleftarrows NiSO_{4\ (aq)} + H_2C_2O_{4\ (aq)} + 2H_2O$ (7)	−31.3
$NiC_2O_4.2H_2O_{(s)} + H_2O \rightleftarrows NiC_2O_{4\ (aq)} + 3H_2O$ (8)	27.2
$NiC_2O_4.2H_2O_{(s)} + H_2SO_{4\ (aq)} \rightleftarrows NiC_2O_{4\ (aq)} + H_2SO_{4\ (aq)} + 2H_2O$ (9)	27.4
$MnC_2O_{4\ (aq)} + H_2SO_{4\ (aq)} \rightleftarrows MnSO_{4\ (aq)} + H_2C_2O_{4\ (aq)}$ (10)	−62.1
$CuC_2O_{4\ (aq)} + H_2SO_{4\ (aq)} \rightleftarrows CuSO_{4\ (aq)} + H_2C_2O_{4\ (aq)}$ (11)	−33.2
$Cu_{(s)} + 2H_2SO_{4(aq)} \rightleftarrows CuSO_{4\ (aq)} + SO_{2\ (g)} + 2H_2O$ (12)	−62.7
$3H_2C_2O_{4\ (aq)} + H_2O_2 \rightleftarrows 6CO_{2\ (g)} + 2H_{2\ (g)} + 2H_2O$ (13)	−658.8

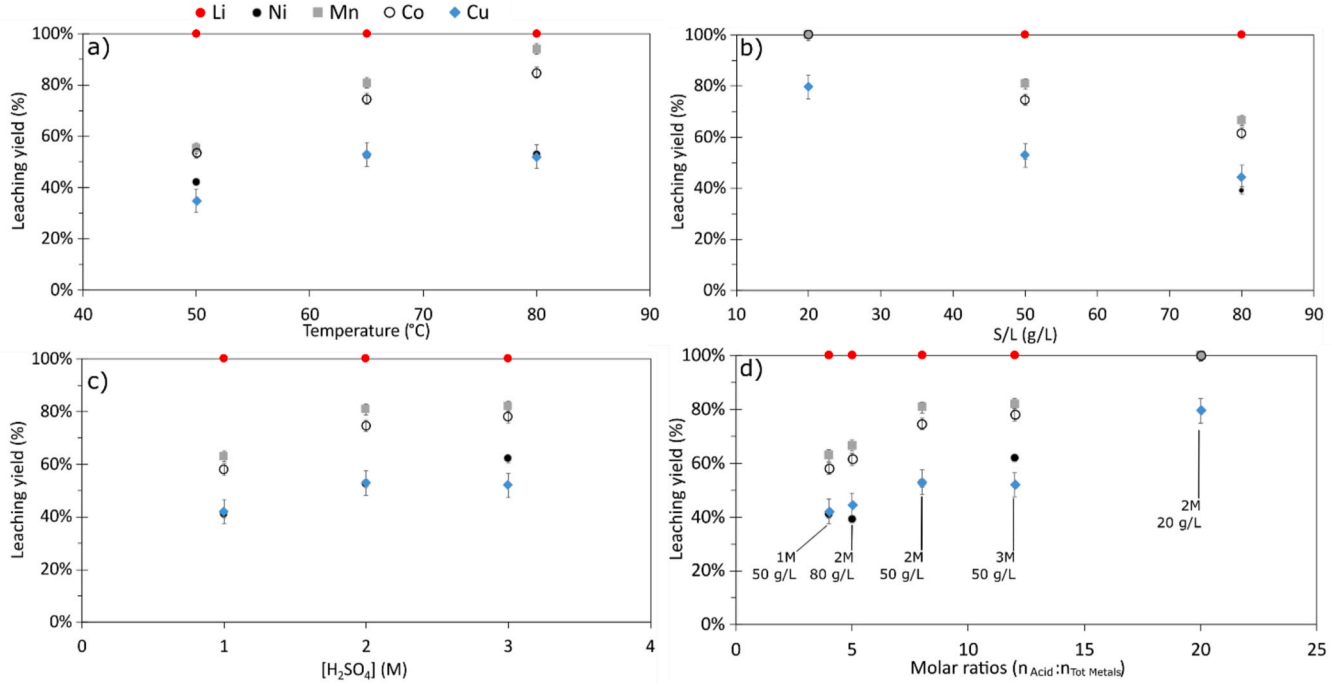

Fig. 1. Preliminary experiments of Leaching II with H_2SO_4 of the residue from Leaching I (V = 50 mL–300 rpm) – Leaching yield for all elements a) Effect of the temperature (S/L ratio = 50 g/L, $[H_2SO_4]$ = 2 M, t = 60 min), b) Effect of the S/L ratio ($[H_2SO_4]$ = 2 M, T = 65 °C, t = 60 min, c) Effect of the acid concentration (S/L ratio = 50 g/L, T = 65 °C, t = 60 min), and d) Effect of the molar ratios between n_{Acid}:$n_{TotalMetals}$.

the dissolved oxalate-associated species, is not spontaneous; this is predictable as they are known to be insoluble. Hence, it reinforces the hypothesis that the dissolution depends on the amount of acid provided to solubilize the oxalate, which then forms a metal sulfate complex in solution. This transformation seems to be the driving force of the dissolution. Also, note that the reaction between the soluble oxalate compound and H_2SO_4 is spontaneous.

Apart from the dissolution reactions, it is essential to mention that some side reactions are possible, such as the degradation of OA molecules with concentrated H_2SO_4, resulting in the formation of CO_2 gas, or the presence of fluorine, which could interfere and create other species with the elements.

3.1.2. Scale-up

The Leaching II operation was scaled up to a reactor volume of 1 L. From the preliminary experiments, the agitation (300 rpm), temperature (65 °C), and molarity of H_2SO_4 (2 M) were fixed. The leaching duration was extended to 2 h instead of 1 to ensure that the system reaches equilibrium by the end of the operation, and to confirm that reaction kinetics are not limiting the process. The S/L ratios were varied to better observe the behavior of all metals and identify the driving force for the dissolution. The leaching yield and concentration in the solution after 120 min are shown in Fig. 2 and for the individual elements in Fig. S3.

As in section 3.1.1, the general observation is that the higher the S/L ratios (lower molar ratios), the lower the dissolution yield. Li is almost fully recovered regardless of the applied conditions. More than 90 % of the Co, Ni, and Mn are dissolved for a molar ratio higher than 20, except for Cu, which is dissolved at about 70 % under the same conditions. Cu would need oxidative conditions to dissolve more efficiently, as it remains in the residue mainly as metallic Cu. Although the reaction is thermodynamically spontaneous (Table 2), it usually needs the addition of an oxidative agent to facilitate the recovery. However, using any oxidative source should be avoided here as it would enhance $H_2C_2O_4$ degradation, as seen in Equation (13). When the molar ratio is 5 (S/L ratios of 80 g/L), Co and Mn recovery decreases by about 30 %. This decrease in recovery is rather proportional to the reduction of molar ratios. Moreover, their concentration in the leachate increases promptly, 4.5 and 3.4 g/L, respectively, against 1.8 and 1.2 g/L after leaching at 20 g/L.

Ni dissolution does not follow the same trend as Mn and Co; its recovery and concentration are distinct when the molar ratio is lower than 20. After 120 min of leaching, Ni concentration reaches a plateau at about 1.5 g/L under most studied S/L conditions (Fig. 2b). In fact, Ni concentration initially goes above this level (up to 2 g/L for the higher S/L ratio) but gradually drops after 30 min of leaching (Fig. 2c). Thus, it appears that Ni reaches a solubility limit at around 1.3 g/L when the acid-to-metal stoichiometry is lower than 20. However, when looking at the solubility data, the $NiSO_4$ compound is highly soluble in water (solubility of 40 g/100 g H_2O at 20 °C [36]). This suggests that Ni exists as oxalate in the solution and has a solubility of about 1 g/L (in a solution of 2 M H_2SO_4 at 65 °C). This observation contradicts the thermodynamic data, which indicate that sulfates should form.

3.1.2.1. Leaching residue characterization. The metal composition of each leaching residue is provided in Table S2 and is consistent with the measured solution concentrations. The leaching residues were further analyzed by FT-IR (Fig. S4a) and XRD (Fig. 3a).

After leaching at 20 g/L, graphite is detected as the main phase remaining in the solid. Additional diffraction peaks are also observed; however, due to their very low intensity, a clear identification of phases is hindered. Based on the ICP-determined composition (Table S2), which shows the presence of Co, Ni, and Cu, these diffraction peaks are attributed to Cu and to possible CoO and NiO phases (Fig. S5a). Another diffraction peak at 18.7° 2θ can also be seen. This peak suggests the presence of a residual oxalate phase resulting from incomplete H_2SO_4 leaching. Another possibility is the presence of a de-lithiated NMC-like phase (containing only Co and Ni) remaining from the initial BM (Fig. S5b). In our previous study [37], we determined that OA leaching occurs at the surface and in the bulk of NMC particles, potentially leading to the entrapment of unreacted NMC during oxalate precipitation, which was further leached by H_2SO_4 during Leaching II. The presence of residual oxides may be due to the absence of added reducing agents during leaching, which are typically used in inorganic acid leaching [38].

For the residues obtained after leaching at 40 g/L and 80 g/L, the diffraction patterns differ, and the peaks can be assigned to a graphite phase and to oxalates, consistent with the IR spectra (Fig. S4a). However, unlike the residue from Leaching I, which consists of a single (Co,Ni,Mn)$C_2O_4 \cdot 2H_2O$ phase, a peak splitting can now be observed (zoom, in Fig. 3a). A peak splitting was also observed by Wang et al., who showed that the mixture of CoC_2O_4 and NiC_2O_4 results in a hybrid phase instead of a solid solution phase [39]. This suggests the presence of two distinct oxalate phases after Leaching II. The identification of these phases was done with the help of a Pawley refinement (Fig. S6), and the results are provided in Table S3. The first oxalate phase corresponds to $NiC_2O_4 \cdot 2H_2O$ for which the determined lattice parameters are in good agreement with the ones reported in the literature [40]. The other oxalate could be identified as a disordered (Co,Ni,Mn)$C_2O_4 \cdot 2H_2O$ phase,

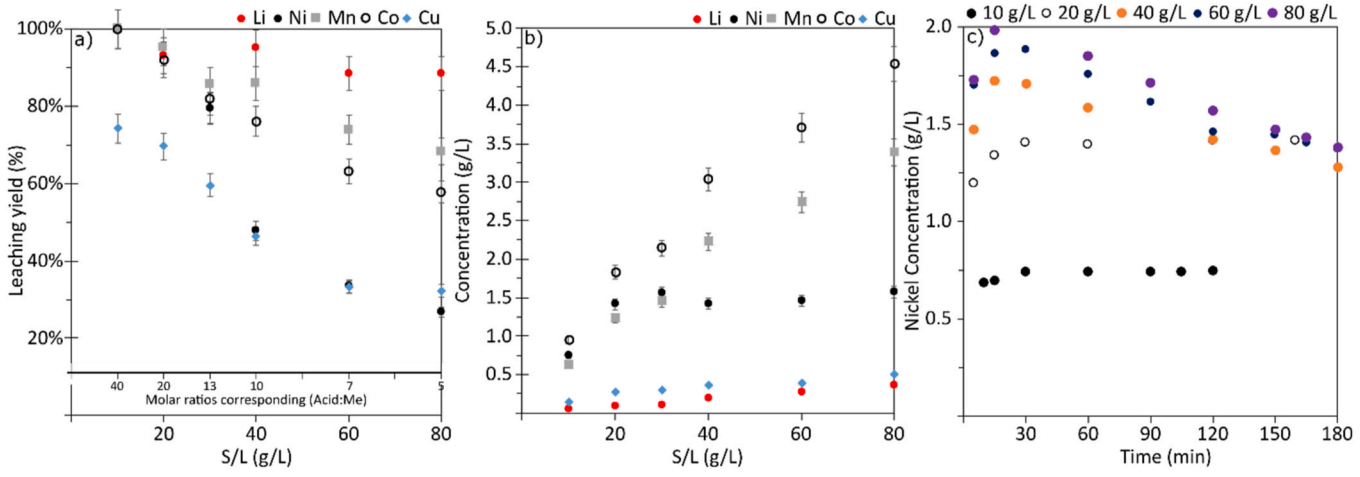

Fig. 2. Scale-up experiments of sulfuric acid leaching II of the residue I (V = 1 L – 300 rpm) - a) Leaching yield of every metals, b) the corresponding metal concentration in the leaching solution II (T = 65 °C, $[H_2SO_4]$ = 2 M, t = 120 min) at different S/L ratios, and c) Nickel concentration during the different leaching experiments (T = 65 °C, $[H_2SO_4]$ = 2 M, t = 120 min).

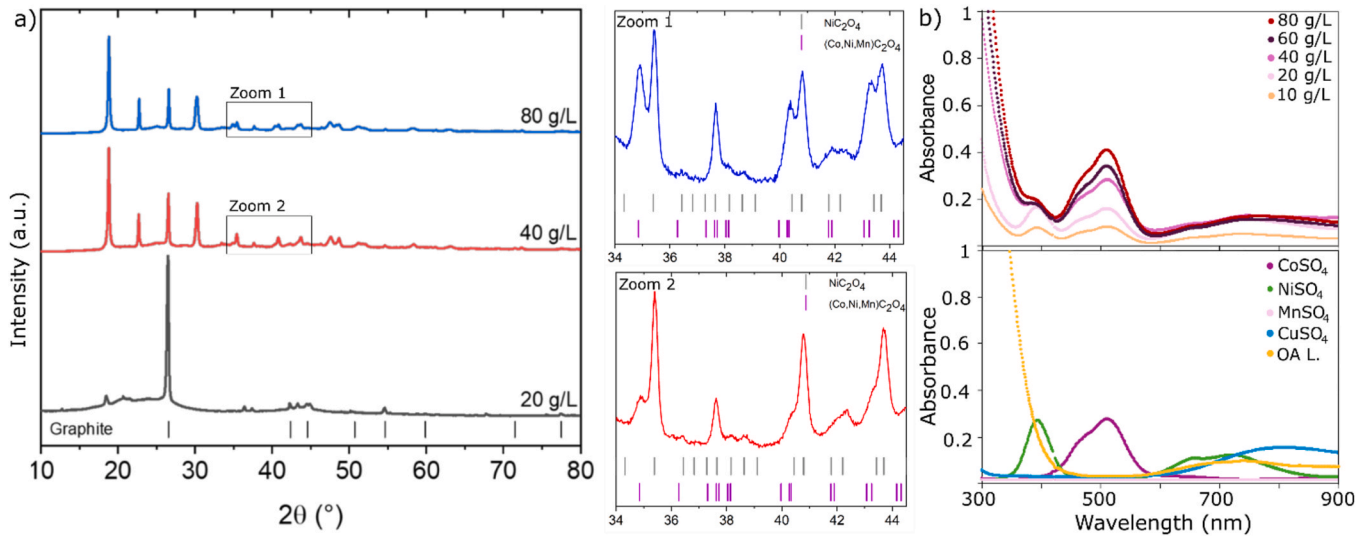

Fig. 3. a) XRD pattern of the leaching residue II at S/L ratios of 20, 40 and 80 g/L with two zooms in the pattern in the region 34–45° 2θ and b) UV–Vis spectra of the resulting leaching solutions (T = 65 °C, [H_2SO_4] = 2 M, t = 120 min, 300 rpm agitation) at different S/L ratios (top) and of standard sulfate solution (concentration corresponding to the concentration in the leaching solution determined by ICP: [Co] = 3.58 g/L, [Ni] = 0.72 g/L, [Mn] = 2.99 g/L, and [Cu] = 0.26 g/L) and the OA leaching solution (marked OA L.) (bottom).

similar to the one used as the starting material for Leaching II. However, the lattice parameters of this new mixed metal oxalate are slightly decreased, which can be attributed to the H_2SO_4 leaching and the associated changes in the composition.

Hence, this indicates that while the (Co,Ni,Mn)C_2O_4 phase from Leaching I dissolves, a new NiC_2O_4 phase forms once a threshold concentration of 1.3 g/L in solution (Fig. 2) is reached. At that point, it appears that the dissolved Ni species reacts with the OA in solution, becomes insoluble and reprecipitates as Ni-oxalate. Moreover, the mixed metal oxalate peaks are less pronounced in the 40 g/L residue than in the 80 g/L residue. This means that as the S/L ratio increases, the (Co,Ni,Mn)C_2O_4 · 2H2O oxalate phase reacts less, reducing the degree of leaching completion.

3.1.2.2. Leaching solution characterization. To better understand in which speciation Ni is present in the leachate solutions, they were studied using spectroscopic techniques. The UV/Vis spectra of the leachate solutions are compared to those of the standard TM sulfate solutions (Fig. 3b). These references were prepared by dissolving the respective sulfate salt in water to obtain a metal concentration corresponding to the one in the leachate solution at 80 g/L. $NiSO_4$ shows a band centered around 390 nm as well as a broad band with two maxima centered around 650 nm and 730 nm, respectively. $CoSO_4$ shows a multiple band at 510 nm, $CuSO_4$ presents a broad band centered at 800 nm, and for $MnSO_4$, no bands can be evidenced.

In comparison, the leaching solutions show the same spectral features as these standard sulfate solutions. In all leachates, the Ni^{2+} absorbance band around 390 nm as well as the Co^{2+} multiple band centered at 510 nm can be clearly evidenced. This confirms the presence of Co and Ni sulfates in the solution, also in agreement with the FT-IR spectra (Fig. S4b). Moreover, above 770 nm, the absorbance in the leachates does not decrease as it is the case in the $NiSO_4$ reference but rather shows similar spectral features as the $CuSO_4$ reference, indicating the presence of Cu^{2+} ions in the leaching solution. Additionally, an intense absorbance band starting at 350 nm can be seen and is assigned to the presence of OA in the solution, which is formed as a by-product during the leaching process.

Regarding the absorbance band intensities, they increase proportionally with the S/L ratio, particularly those assigned to the Co^{2+} species. This is consistent with an increasing metal concentration in the leachates as presented in Fig. 2b. Interestingly, for the Ni^{2+} species, the band at 390 nm presents a maximum absorbance at around 0.2 for all solutions, except the 10 g/L leachate. This confirms the dissolution limit, as already observed in Fig. 2b. Hence, Ni exists primarily as sulfate in the solution, and its recovery limitation could be in the solubility limit of an intermediate product instead of the final one. The reaction presented in Equation (6) is not complete, even if thermodynamics considers it spontaneous. Beyond the solubility argument, some limitations could arise from the amount of acid provided or the kinetics.

Equation (14) expresses the proposed leaching mechanism of the mixed metal oxalate with H_2SO_4. The oxalate phase is depleted of the three elements more or less simultaneously leading to the formation of metal sulfates in solution. However, a large excess of acid is required to complete the reaction. If the S/L ratio is too high, a new oxalate phase containing mainly Ni is formed due to the maximum dissolution of Ni under the studied conditions, as revealed by Equation (15).

$$(Co_xNi_yMn_z)C_2O_4 \cdot 2H_2O + H_2SO_4 \rightleftarrows x\,CoSO_4 + y\,NiSO_4 + z\,MnSO_4 + H_2C_2O_4 + 2H_2O \quad (14)$$

$$NiSO_4 + H_2C_2O_4 \rightleftarrows NiC_2O_4 + H_2SO_4 \quad (15)$$

Different potential strategies for the recycling process can be considered. As highlighted above, close to 100 % recovery of all material involves the production of a low-concentration solution, while higher S/L ratio decreases the recovery but produces a concentrated solution. To maximize the recovery of all elements, two alternatives can be proposed (as seen in Fig. S7a).

- The leaching operation is run at an S/L ratio of 20 g/L, leading to a recovery of close to 95 % but with low metal concentration (approximately 1.5 g/L). This S/L ratio is relatively low for industrial standards, as it will involve larger chemical consumption and longer processing time for the same mass of waste processed [41,42]. The mass balance for this strategy is provided in Fig. S7b.
- The process could be done in several stages: a first leaching with an S/L ratio of 40 g/L and a second step at 20 g/L to overcome the solubility of Ni and reach 100 % recovery. This alternative was tested in the lab, and the overall recovery exceeded 95 % for all elements, yielding two solutions with different concentrations, giving potential for the precipitation of different CAM precursors.

For the rest of the study, only the first option was considered, as it

was evaluated to have stronger industrial potential than the two-stage leaching process.

3.2. Towards the production of CAM precursors

3.2.1. Impurity concern – Removal of Cu

The major contaminant in the solution regarding its potential for cathode material precursor is Cu [35,43–48]. It is worth noting that Li is not seen as an impurity, as in very low quantities, it will not affect the NMC synthesis [35,46]. On the contrary, it could participate depending on the synthesis process chosen in the end. Metallic Cu is known to have a negative effect on the electrochemical performance of the regenerated NMC materials. A moderate amount of Cu ions could promote particle nucleation, enhance primary particle growth, and reduce cation mixing in the NMC cathode. However, an excess of Cu would degrade electrochemical performance [44,45]. With that in mind, Cu must be removed and left only at a trace level. The limit of acceptance would vary depending on the desired performance, based on reported values, the limit was set at 5 ppm in this work [43,47,48]. Precipitation techniques cannot be used as other elements could co-precipitate, and minimizing losses is crucial in this process. Hence, solvent extraction (SX) is the technology of choice for this separation. It allows a selective and effective metal recovery from an aqueous solution, even at trace levels. Cu extraction has been well-documented over the years. However, its extraction from a sulfuric aqueous matrix accompanied by residual OA has not yet been demonstrated. OA still has a complexing ability and could form some soluble anionic Cu oxalate form, which could resist the extraction system.

The extractant selected is Acorga M5640, a commercial extractant widely used in the industry because of its high selectivity on Cu. It is an acidic extractant expected to follow Equation (16). Hence, Cu extraction efficiency is significantly impacted by the pH of the feed solution and the equilibrium pH. For instance, optimal extraction conditions for Acorga M5640 were found at an equilibrium pH of 2.5, where nearly 92 % of Cu was extracted [49,50]. Other authors report that about 85 % extraction could be achieved from a feed containing Cu and Zn in perchloric acid at an initial pH of 1 [51]. To optimize Cu extraction, equilibrium pH control would be recommended (e.g., adding a base to neutralize the leachate solution, such as NaOH) to shift the equilibrium towards the extractable complex formation. The natural pH of the leachate solution is below 0.

$$Cu^{2+} + \overline{2\,HE} \rightleftarrows \overline{CuE_2} + 2\,H^{+} \quad (16)$$

3.2.2. pH control

Prior to performing the extraction test, the pH of the solution was adjusted to evaluate its influence on the oxalate solubility while removing acidity and therefore the apparition of a solid phase. The presence of a solid (3rd phase) during SX is highly undesirable, as it can interfere with phase separation, reduce extraction efficiency, and complicate downstream processing. For this reason, systems exhibiting solid formation during extraction are typically avoided. Therefore, these pH adjustment experiments are essential for the rest of the study, and the tests were performed on the leachate solution (S/L ratio = 20 g/L).

The variation of concentrations after adjusting and controlling the pH are depicted in Fig. 4a and Fig. S8. It shows that the elements are unstable in the solution; after a couple of hours, the metal concentration is decreased by half, and a white powder is visible at the bottom of the reactor. The XRD patterns (Fig. 4c) obtained after pH = 2 and 4 precipitation reveal that oxalates are formed. The results of the Pawley refinement are provided in Fig. S9 and Table S4. These precipitates are

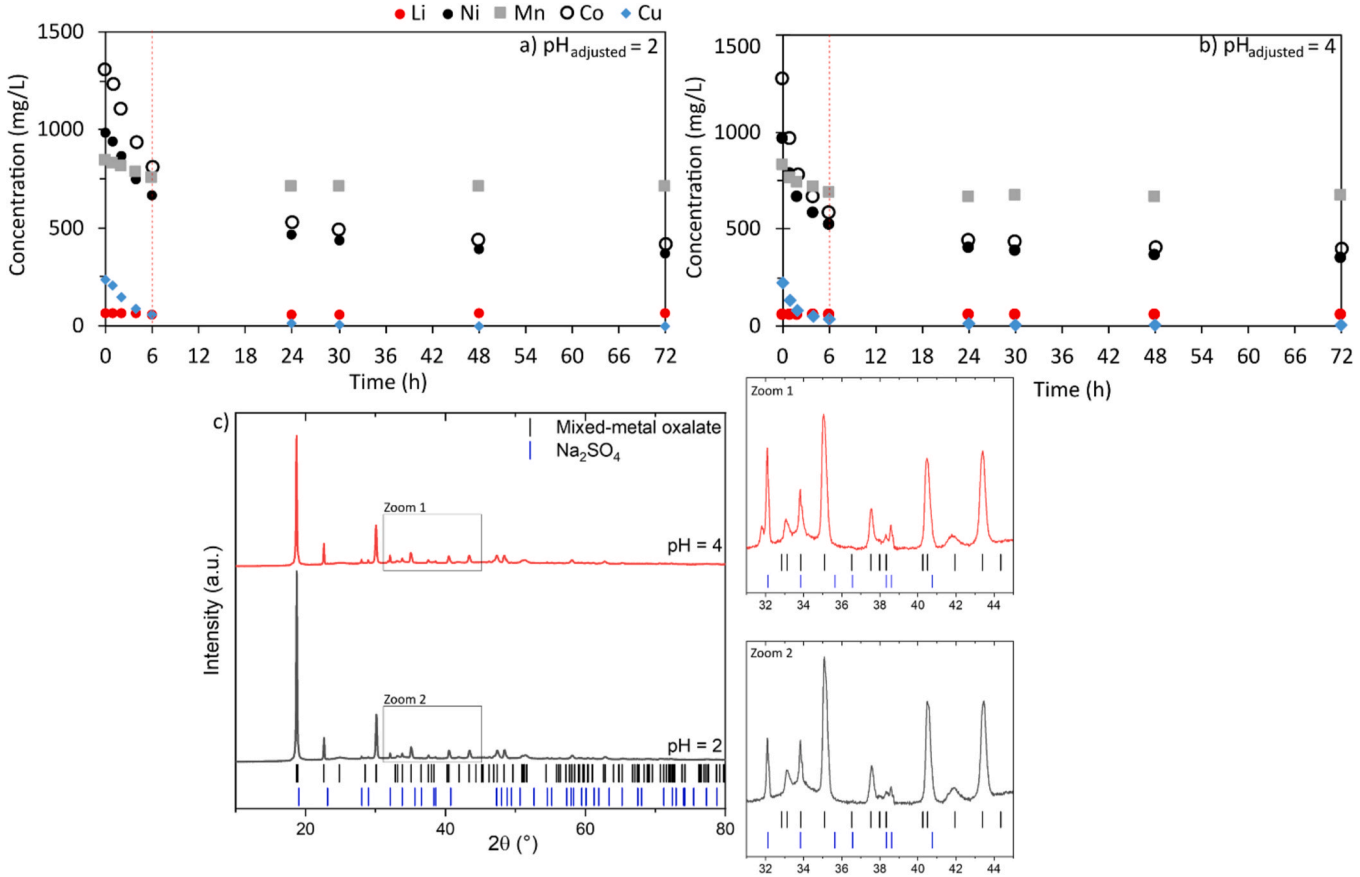

Fig. 4. Precipitation of the elements from the leaching solution II (20 g/L, 2 M, 65 °C, 120 min) – Evolution of the metal concentration after adjusting the pH a) at 2, b) at 4, and c) XRD pattern of precipitates obtained at pH = 2 and 4 and a zoom in each pattern between 2θ = 31–45°.

again a single disordered mixed metal oxalate phase with a general formula $(Co,Ni,Mn)C_2O_4 \cdot 2H_2O$ (no peak splitting observed). The lattice parameters are close to the ones expected for the single-metal oxalates [40] and can be considered as a mean of the individual oxalate lattice parameters. This further confirms that all elements co-precipitate. It should also be noted that Na_2SO_4 (PDF: 00-037-1465) forms as a byproduct of the process, which should be possible to remove by adding a washing step during the optimization of the precipitation of the CAM precursor.

Precipitation occurs even at pH 1, as seen in Fig. S8, which poses a significant challenge for Cu removal as the equilibrium pH cannot be controlled during SX due to the potential 3rd phase formation. Additional pH adjustment tests show that a pH of 0.4 avoids any precipitation, and metals remain stable in the solution. Hence, the pH of the solution was fixed at that initial value before continuing SX investigation.

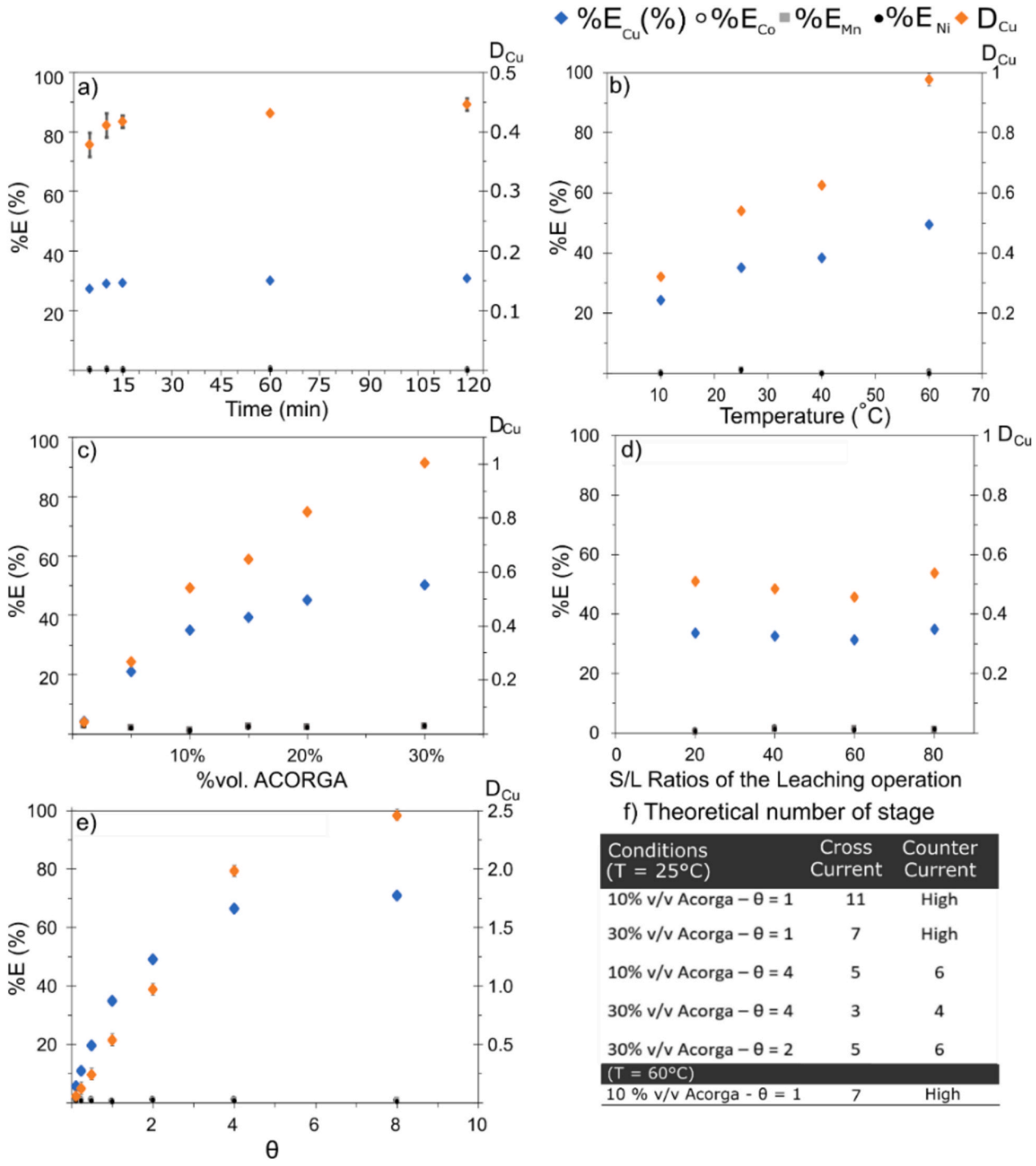

Conditions (T = 25°C)	Cross Current	Counter Current
10% v/v Acorga – θ = 1	11	High
30% v/v Acorga – θ = 1	7	High
10% v/v Acorga – θ = 4	5	6
30% v/v Acorga – θ = 4	3	4
30% v/v Acorga – θ = 2	5	6
(T = 60°C)		
10 % v/v Acorga - θ = 1	7	High

Fig. 5. Extraction yield (blue) and distribution coefficient (orange) of Cu and extraction yield for the other elements – a) Effect of the mixing time (θ = 1; T = 25 °C; 10 % v/v ACORGA M5640/ESAID), b) Effect of the temperature (θ = 1; t = 30 min; 10 % v/v ACORGA M5640/ESAID), c) Effect of the Acorga M5640 concentration (θ = 1; t = 30 min, T = 25 °C), d) Effect of the leaching solution composition (θ = 1; T = 25 °C; t = 30 min; 10 % v/v ACORGA M5640/ESAID), e) Effect of θ (T = 25 °C; t = 30 min; 10 % v/v ACORGA M5640/ESAID) and f) Theoretical number of stage under different conditions – High is higher than 12. (For interpretation of the references to colour in this figure legend, the reader is referred to the Web version of this article.)

Although the oxalate precipitation complicates the Cu separation via SX, it may offer a valuable advantage for the whole process. Specifically, it opens the possibility of directly producing the mixed metals oxalates from the recycled solution. These compounds are already known to have substantial potential as precursors for CAM or as energy materials in some storage devices [52–55], making the proposed process technically promising. Additionally, if metal oxalates are removed from the solution, the sulfuric acid solution could be regenerated and reused in the process which could be economically favored.

3.2.3. Solvent extraction batch experiments

As demonstrated, equilibrium pH control is not an option in this process as precipitation may occur [56]. For the SX study, the leaching solution at 80 g/L is used as it presents the highest concentration of Cu. At low feed pH, the extraction is more sensitive to variations in the feed Cu concentration [50,57]. Thus, all leachate solutions will be tested under optimum conditions. Before extraction, all solutions had their pH adjusted to 0.4. The extraction yield of Cu, Mn, Co, and Ni and D-value of Cu are shown in Fig. 5, and the selectivity of Acorga M5640 for Cu is demonstrated. Phase separation is easily achieved, and the organic phase changes from transparent to golden once Cu is loaded.

Equilibrium is reached after 15 min (Fig. 5a), and 35 % of Cu is extracted. This low extraction level is expectable as the feed solution has a quite low pH (0.4), hindering the extraction reaction, as explained above. Additional parameters are investigated to increase Cu recovery and shift the equilibrium towards extraction. The very low co-extraction of the other valuable metals is a key factor in the operation. Scrubbing will not be required, which would have complicated the purification process and increased operational costs. A time of 30 min is selected for further investigations.

Temperature impacts the extraction yield; it increases from 35 % at 25 °C to 49 % at 60 °C (Fig. 5b). This 14 % increase is not surprising as the extraction mechanism with Acorga M5640 is an endothermic reaction, hence, higher temperature shifts the equilibrium toward complex formation between the metal ions and the extractant [50,51]. The temperature also affects the physical properties of the organic phase, such as viscosity and density, which are not limiting in this case. Hence, experiments were performed at 25 °C, as this decreases the need for energy and the complexity of the process.

The parameter that most impacts Cu recovery is the concentration in Acorga M5640 (given in volume percentage in ESCAID). For 5 % *v/v* Acorga M5640, the extraction is at 21 %, while it is about 50 % for a concentration of 30 % *v/v*. Co, Mn, and Ni co-extraction is not strongly affected and keeps an average value of about 2 % (Fig. 5c). An extraction of 50 % is low, considering the applied condition, but not surprising considering the very low concentration of the element in the solution. As mentioned above, the pH is extremely low, which can affect the extraction mechanism, i.e., it can lead to the extractant protonation and affect the equilibrium.

In the same way as the Acorga M5640 concentration, increasing θ largely favors the extraction (Fig. 5e). Extraction capacities are identical depending on the leachate solution used as feed (Fig. 5d), which was essential in the development process. All experiments are batch experiments, and multistage operations will be needed to achieve a satisfying separation of Cu (under 5 ppm, so above 99 % efficiency percentage). Equation (15) represents another simplified expression of the extraction percentage in the case of crosscurrent extraction. Equation (16) is the expression of the percentage extracted for countercurrent extraction; it is also known as the Kremser equation. They can both be used to determine the theoretical number of stages (n) needed.

$$\%E_M = 1 - \frac{1}{(1 + D_M \,.\, \theta)^n} \tag{15}$$

$$\%E_M = 1 - \frac{D_M \,.\, \theta - 1}{D_M \,.\, \theta^{n+1} - 1} \tag{16}$$

Data obtained for the batch experiments (D-values) were computed to obtain the theoretical number of stages needed to achieve the 99 % of extraction needed; results are reported in Fig. 5f. Cross-current extraction would require fewer stages, but it consumes a large volume of organic material as fresh organic solution is distributed at each stage. Counter-current extraction would need more stages and a minimum θ of 2 for effective extraction and is industrially preferred. With this prediction, we would still recommend its usage as less volume is spent. Moreover, increasing the temperature, despite the increase of energy needed, can significantly reduce the number of stages (4 stages less when the temperature is increased from 25 to 60 °C). Additional experimental tests and validation would be needed to validate this theoretical number of stages.

Additionally, stripping experiments were performed to validate the unloading of Cu. They were performed with 2 M H_2SO_4 at 25 °C and θ at 0.5. For all organics solutions tested, 100 % of the Cu could be stripped with high purity (>99.5 % Cu).

4. Conclusions

A novel LiB recycling process has been investigated to support circular economy goals and reduce reliance on virgin materials. The method begins with selective lithium recovery using OA leaching, dissolving 85 % of Li and all Al, which minimizes downstream contamination.

The remaining residue (containing TM oxalate, graphite, and Cu) is then leached with sulfuric acid. A one-stage leaching (20 g/L) with 2 M H_2SO_4 at 65 °C for 120 min recovers over 95 % of Co, Ni, Mn, and 70 % of Cu. After leaching, graphite is recovered by filtration. Higher S/L ratios lead to the presence of two oxalate phases in the residue: one enriched in Ni, and one containing all TM elements.

Cu is removed via solvent extraction using Acorga M5640 (30 % v/v Acorga M5640 in ESCAID for 30 min, at 25 °C, with θ = 4 and 4 countercurrent stages), achieving concentrations below 5 mg/L. The final purified solution (1.83 g/L of Co, 1.41 g/L of Ni, 1.23 g/L of Mn and 0.266 ppm of Cu) is suitable for synthesizing NMC111 oxalate precursors. This process offers a sustainable, high-yield alternative to conventional sourcing. However, the solvents recyclability remains a challenge and will be addressed in future research.

CRediT authorship contribution statement

Léa Marie Jacqueline Rouquette: Writing – original draft, Investigation, Data curation, Conceptualization. **Laura Altenschmidt:** Writing – original draft, Investigation, Data curation, Conceptualization. **Camille Travert:** Writing – original draft, Investigation, Data curation. **Andrea Locati:** Writing – review & editing. **William R. Brant:** Writing – review & editing, Supervision. **Martina Petranikova:** Writing – review & editing, Supervision, Funding acquisition, Conceptualization.

Declaration of competing interest

The authors declare the following financial interests/personal relationships which may be considered as potential competing interests: Martina Petranikova reports financial support was provided by Swedish Energy Agency. Martina Petranikova reports a relationship with Sweden's Innovation Agency that includes: funding grants. If there are other authors, they declare that they have no known competing financial interests or personal relationships that could have appeared to influence the work reported in this paper.

Acknowledgments

This research was funded by ÅForsk (grant number: 19-695) and Battery fund (grant number: P2021-90022). The authors would like to acknowledge the support of Volvo Car AB for providing samples.

Appendix A. Supplementary data

Supplementary data to this article can be found online at https://doi.org/10.1016/j.powera.2026.100201.

Data availability

Data will be made available on request.

References

[1] International Energy Agency Recycling of Critical Minerals - Strategies to Scale up Recycling and Urban Mining, 2024.
[2] International Energy Agency (IEA), Global EV Outlook 2022 Securing Supplies for an Electric Future, 2022. Paris.
[3] L. Dahllöf, M. Romare, A. Wu, Mapping of Lithium-Ion Batteries for Vehicles - a Study of their Fate in the Nordic Countries, vol. 1, Springer, Copenhangen, Danmark, 2016. ISBN 9783319191072.
[4] G. Harper, P.A. Anderson, E. Kendrick, W. Mrozik, P. Christensen, S. Lambert, D. Greenwood, P.K. Das, M. Ahmeid, Z. Milojevic, et al., Roadmap for a sustainable circular economy in lithium-ion and future battery technologies, J. Phys.: Energy (2022), https://doi.org/10.1088/2515-7655/acaa57.
[5] European comission critical raw Material (CRM), Available online: https://single-market-economy.ec.europa.eu/sectors/raw-materials/areas-specific-interest/critical-raw-materials_en. (Accessed 30 April 2024).
[6] N. Hayagan, C. Aymonier, L. Croguennec, G. Philippot, A Holistic Review on the Direct Recycling of Lithium- Ion Batteries from Electrolytes to Electrodes, 2024, https://doi.org/10.1039/D4TA04976D.
[7] J. Qing, G. Zhang, L. Zeng, W. Guan, Z. Cao, Q. Li, M. Wang, Y. Chen, S. Wu, Deep fluoride removal from the sulfate leaching solution of spent LIBs by complexation extraction with Al3+ loaded solvent, Sep. Purif. Technol. 305 (2023) 122343, https://doi.org/10.1016/j.seppur.2022.122343.
[8] M. Rinne, H. Elomaa, A. Porvali, M. Lundström, Simulation-Based life cycle assessment for hydrometallurgical recycling of mixed LIB and NiMH waste, Resour. Conserv. Recycl. 170 (2021), https://doi.org/10.1016/j.resconrec.2021.105586.
[9] K. Binnemans, P. Tom, The twelve principles of circular hydrometallurgy, J. Sustain. Metall. 9 (2023) 1–25, https://doi.org/10.1007/s40831-022-00636-3.
[10] European parliament and the council of the european union regulation (EU) 2023/1542 - batteries and waste batteries, Amending Directive 2008/98/EC and Regulation (EU) 2019/1020 and Repealing Directive 2006/66/EC vol. 66, 2023.
[11] M. Armand, P. Axmann, D. Bresser, M. Copley, K. Edstr, C. Ekberg, D. Guyomard, B. Lestriez, P. Nov, M. Petranikova, et al., Lithium-ion batteries – current state of the art and anticipated developments, Power Sources 479 (2020) 26, https://doi.org/10.1016/j.jpowsour.2020.228708.
[12] J. Heelan, E. Gratz, Z. Zheng, Q. Wang, M. Chen, D. Apelian, Y.A.N. Wang, Current and Prospective Li-Ion Battery Recycling and Recovery Processes, vol. 68, 2016, pp. 2632–2638, https://doi.org/10.1007/s11837-016-1994-y.
[13] F. Larouche, F. Tedjar, K. Amouzegar, G. Houlachi, P. Bouchard, G.P. Demopoulos, K. Zaghib, Progress and status of hydrometallurgical and direct recycling of Li-Ion batteries and beyond, Materials 13 (2020), https://doi.org/10.3390/ma13030801.
[14] J. Zhang, Application of Hydrometallurgy in Spent Lithium-Ion Battery Recycling, Elsevier Inc., 2022. ISBN 9780323911344.
[15] J. Jung, P.-C. Sui, J. Zhang, Hydrometallurgical Recycling of Lithium-Ion Battery Materials, 2023. ISBN 9781032216027.
[16] W. Lv, Z. Wang, H. Cao, Y. Sun, Y. Zhang, Z. Sun, A critical review and analysis on the recycling of spent lithium-ion batteries, ACS Sustain Chem Eng 6 (2018) 1504–1521, https://doi.org/10.1021/acssuschemeng.7b03811.
[17] P. Meshram, A. Mishra, Abhilash, R. Sahu, Environmental impact of spent lithium ion batteries and green recycling perspectives by organic acids – a review, Chemosphere 242 (2020) 125291, https://doi.org/10.1016/j.chemosphere.2019.125291.
[18] H. Wang, B. Friedrich, Development of a highly efficient hydrometallurgical recycling process for automotive Li–Ion batteries, J. Sustain. Metall. 1 (2015) 168–178, https://doi.org/10.1007/s40831-015-0016-6.
[19] W. Yu, Y. Guo, S. Xu, Y. Yang, Y. Zhao, J. Zhang, Comprehensive recycling of lithium-ion batteries: fundamentals, pretreatment, and perspectives, Energy Storage Mater. 54 (2023) 172–220, https://doi.org/10.1016/j.ensm.2022.10.033.
[20] D. Amalia, P. Singh, W. Zhang, A.N. Nikoloski, A review of pretreatment methods for spent lithium-ion batteries to produce black mass–comparison of processes of Asia Pacific recyclers, Miner. Process. Extr. Metall. Rev. (2024), https://doi.org/10.1080/08827508.2024.2367420.
[21] L.F. Guimarães, A.B. Botelho Junior, D.C.R. Espinosa, Sulfuric acid leaching of metals from waste Li-Ion batteries without using reducing agent, Miner. Eng. 183 (2022), https://doi.org/10.1016/j.mineng.2022.107597.
[22] P. Meshram, B.D. Pandey, T.R. Mankhand, Hydrometallurgical processing of spent lithium ion batteries (LIBs) in the presence of a reducing agent with emphasis on kinetics of leaching, Chem. Eng. J. 281 (2015) 418–427, https://doi.org/10.1016/j.cej.2015.06.071.
[23] M. Petranikova, P.L. Naharro, N. Vieceli, G. Lombardo, B. Ebin, Recovery of critical metals from EV batteries via thermal treatment and leaching with Sulphuric Acid at ambient temperature, Waste Manag. 140 (2022) 164–172, https://doi.org/10.1016/j.wasman.2021.11.030.
[24] A. Chernyaev, B.P. Wilson, M. Lundström, Study on valuable metal incorporation in the Fe–Al precipitate during neutralization of LIB leach solution, Sci. Rep. 11 (2021), https://doi.org/10.1038/s41598-021-02019-2.
[25] Y. Ma, M. Svärd, X. Xiao, J.M. Gardner, R.T. Olsson, K. Forsberg, Precipitation and crystallization used in the production of metal salts for Li-Ion battery materials: a review, Metals 10 (2020) 1–16, https://doi.org/10.3390/met10121609.
[26] A. Chernyaev, J. Zhang, S. Seisko, M. Louhi-Kultanen, M. Lundström, Fe3+ and Al3+ removal by phosphate and hydroxide precipitation from synthetic NMC Li-Ion battery leach solution, Sci. Rep. 13 (2023) 1–12, https://doi.org/10.1038/s41598-023-48247-6.
[27] C. Ekberg, M. Petranikova, Chap 7: lithium batteries recycling, in: Lithium Process Chemistry: Resources, Extraction, Batteries, and Recycling, Elsevier Inc., 2015, pp. 233–267. ISBN 9780128014172.
[28] J. Neumann, M. Petranikova, M. Meeus, J.D. Gamarra, R. Younesi, M. Winter, S. Nowak, Recycling of lithium-ion Batteries—Current State of the art, circular economy, and next generation recycling, Adv. Energy Mater. (2022) 2102917, https://doi.org/10.1002/aenm.202102917.
[29] International Energy Agency (IEA), Recycling of Critical Minerals - Strategies to Scale up Recycling and Urban Mining, 2024.
[30] L.M.J. Rouquette, N. Vieceli, M. Petranikova, Complete and selective recovery of lithium from EV lithium-ion batteries: modeling and optimization using oxalic acid as a leaching agent, Sep. Purif. Technol. 320 (2023), https://doi.org/10.1016/j.seppur.2023.124143.
[31] Léa Rouquette, Laura Altenschmidt, Matea Culina, William R. Brant, M.P. Burçak Ebin, Kinetics Study of the Dissolution of Black Mass Material Using Oxalic Acid as a Leaching Agent - Unpublished Manuscript, 2024.
[32] K.V. Krishnamurty, G.M. Harris, V.S. Sastri, The Chemistry of the Metal Oxalato Complexes, vol. 70, 1960.
[33] Retsch *an Expert Guide to Particle Size Analysis*, 2015.
[34] A.A. Coelho, TOPAS and TOPAS-Academic: an Optimization Program integrating computer algebra and crystallographic objects written in C++, J. Appl. Crystallogr. 51 (2018) 210–218, https://doi.org/10.1107/S1600576718000183.
[35] M. Beak, J. Park, S. Park, S. Jeong, J. Kang, W. Choi, W.S. Yoon, K. Kwon, Understanding the effect of nonmetallic impurities in regenerated cathode materials for lithium-ion battery recycling by tracking Down impurity elements, J Hazard Mater 425 (2022) 127907, https://doi.org/10.1016/j.jhazmat.2021.127907.
[36] David R. Lide CRC Handbook in Chemistry and Physics; Standard R.;.
[37] L.M.J. Rouquette, L. Altenschmidt, M. Culina, W.R. Brant, B. Ebin, M. Petranikova, Kinetics study of the dissolution of black mass material using oxalic acid as a leaching agent, J. Hazard. Mater. Adv. 18 (2025), https://doi.org/10.1016/j.hazadv.2025.100750.
[38] S. Moon, W. Chae, B.M. Jun, Y. Yoon, H. Rho, Comparative study on the leaching behavior of lithium-ion battery black mass using sulfuric and organic acids combined with hydrogen peroxide, Sep. Purif. Technol. 376 (2025), https://doi.org/10.1016/j.seppur.2025.133991.
[39] L. Wang, R. Zhang, Y. Jiang, H. Tian, Y. Tan, K. Zhu, Z. Yu, W. Li, Interfacial synthesis of micro-cuboid Ni0.55Co0.45C2O4 solid solution with enhanced electrochemical performance for hybrid supercapacitors, Nanoscale 11 (2019) 13894–13902, https://doi.org/10.1039/c9nr03790j.
[40] A.N. Puzan, V.N. Baumer, D.V. Lisovytskiy, P.V. Mateychenko, Structure transformations in nickel oxalate dihydrate NiC2O4·2H2O and nickel formate dihydrate Ni(HCO2)2·2H2O during thermal decomposition, J. Solid State Chem. 266 (2018) 133–142, https://doi.org/10.1016/j.jssc.2018.07.005.
[41] Alain Vignes *Extractive Metallurgy 2 - Metallurgical Reaction Processes*, John Wiley and Sons, 2011. ISBN 978-1-84821-287-9.
[42] J.D. Seader, J. Henley Ernest, R.D.K. *Separation Process Principles - Chemical and Biochemical Operations - 3rd Ed.*, John Wiley, 2011. ISBN 978-0-470-48183-7.
[43] O.A. Nasser, M. Petranikova, Review of achieved purities after Li-Ion batteries hydrometallurgical treatment and impurities effects on the cathode performance, Batteries 7 (2021), https://doi.org/10.3390/batteries7030060.
[44] Z.J. Wu, D. Wang, Z.F. Gao, H.F. Yue, W.M. Liu, Effect of Cu substitution on structures and electrochemical properties of Li[NiCo1-XCuxMn]1/3O2 as cathode materials for lithium ion batteries, Dalton Trans. 44 (2015) 18624–18631, https://doi.org/10.1039/c5dt02552d.
[45] R. Zhang, Z. Meng, X. Ma, M. Chen, B. Chen, Y. Zheng, Z. Yao, P. Vanaphuti, S. Song, Z. Yang, et al., Understanding fundamental effects of Cu impurity in different forms for recovered LiNi0.6Co0.2Mn0.2O2 cathode materials, Nano Energy 78 (2020) 105214, https://doi.org/10.1016/j.nanoen.2020.105214.
[46] Q. Wang, R.V. Fox, M. Shi, S.W. Snyder, G.O. Ilevbare, D.M. Ginosar, Electrodialysis: an effective methodology to purify the leachate of spent Li-Ion batteries, Sep. Purif. Technol. 359 (2025), https://doi.org/10.1016/j.seppur.2024.130430.
[47] Queensland University of Technology ABN Li-Ion Battery Cathode Manufacture in Australia - a Scene Setting Project, 2023.
[48] Z. Meng, X. Ma, J. Hou, Y. Zheng, Y. Wang, Impurity impacts of recycling NMC cathodes, Adv. Energy Mater. (2025) 1–25, https://doi.org/10.1002/aenm.202405383, 2405383.
[49] A. Nobahar, A.B. Melka, A. Pusta, J. Paulo, J.D. Carlier, M.C. Costa, A new application of solvent extraction to separate copper from extreme acid mine drainage producing solutions for electrochemical and biological recovery processes, Mine Water Environ. 41 (2022) 387–401, https://doi.org/10.1007/s10230-022-00858-7.
[50] I. Nozari, A. Azizi, An Investigation into the Extraction Behavior of Copper from Sulfate Leach Liquor Using Acorga M5640 Extractant : Mechanism , Equilibrium , and Thermodynamics, 2020, pp. 1673–1680.

[51] A. Deep, P. Kumar, J.M.R. Carvalho, Recovery of copper from zinc leaching liquor using ACORGA M5640, Sep. Purif. Technol. 76 (2010) 21–25, https://doi.org/10.1016/j.seppur.2010.09.015.
[52] J.W. Choi, J. Kim, S.K. Kim, Y.S. Yun, Simple, green organic acid-based hydrometallurgy for waste-to-energy storage devices: recovery of NiMnCoC2O4 as an electrode material for pseudocapacitor from spent LiNiMnCoO2 batteries, J Hazard Mater 424 (2022) 127481, https://doi.org/10.1016/j.jhazmat.2021.127481.
[53] L. Wang, R. Zhang, Y. Jiang, H. Tian, Y. Tan, K. Zhu, Z.L.W. Yu, Interfacial synthesis of micro-cuboid Ni0.55Co0.45C2O4 solid solution with enhanced electrochemical performance for hybrid supercapacitors, Nanoscale (2019), https://doi.org/10.1039/c9nr03790j.
[54] W.A.E. Ang, Y.L. Cheah, C.L. Wong, H.H. Hng, S. Madhavi, One-pot solvothermal synthesis of Co1-XMnxC2O4 and their application as anode materials for lithium-ion batteries, J. Alloys Compd. 638 (2015) 324–333, https://doi.org/10.1016/j.jallcom.2015.02.203.
[55] S. Ghosh, R. Jana, S. Ganguli, H.R. Inta, G. Tudu, H.V.S.R.M. Koppisetti, A. Datta, V. Mahalingam, Nickel–cobalt oxalate as an efficient non-precious electrocatalyst for an improved alkaline oxygen evolution reaction, Nanoscale Adv. 3 (2021) 3770–3779, https://doi.org/10.1039/d1na00034a.
[56] G.M. Ritcey, A.W. Ashbrook, Solvent Extraction - Principles and Applications to Process Metallurgy, Elsevier Science Publisher, 1984. ISBN 0-444-41751-2.
[57] M. Hosseinzadeh, J. Petersen, A. Azizi, Solvent extraction studies of copper from a heap leach liquor using mextral 5640H, Minerals 12 (2022) 1–14, https://doi.org/10.3390/min12101322.